



# Mechanical and optical design for assembly of vascular endothelial cells using laser guidance and tweezers

H. Hocheng\*, C. Tseng

Department of Power Mechanical Engineering, National Tsing Hua University, 101, Section 2, Kuang-Fu Road, Hsinchu, Taiwan 30013, ROC

## ARTICLE INFO

### Article history:

Received 14 February 2008

Received in revised form 2 April 2008

Accepted 2 May 2008

### OCIS:

350.4855

140.7010

160.1435

## ABSTRACT

Laser is applied to guide and tweeze the vascular endothelial cells for assembly. The system is composed of three modules: laser guidance, micro channels and laser tweezers. The micro channel includes the assembly area, main channel and branch channels. The optical module is equipped with laser source, beam splitter, reflectors and lenses. The endothelial cells are delivered to main channel and guided through branch channel to the assembly area by laser. The optical tweezers then move the cells to the proper position. The design of optical modules is conducted for the maximum capability of manipulating cells. The micro channel is designed based on fluid mechanics to minimize the fluidic disturbance to the cells in the assembly area, and is fabricated by photo lithography. Polystyrene micro beads and endothelial cells are successfully guided and tweezed by this approach. The associated escape velocity and dragging force are investigated.

© 2008 Elsevier B.V. All rights reserved.

## 1. Introduction

In spite of the average human life getting longer, the organs aged with time. Cardiovascular disease such as atherosclerosis is one of the most serious chronic diseases in the modern society. Since the successful use of single laser to manipulate micro particle [1], researchers start to investigate the mechanical model and further applications of optical tweezers [2,3]. Because optical tweezers can move particles and microorganism without contact, it becomes a powerful tool for biological research.

Multiple optical tweezers can further control large amount of particles at the same time. They are achieved by laser array [4], beam splitters [5], spatial light modulator [6,7] and micro mirror array [8]. Laser array uses parallel light source to produce light spots on the objective plane. This method can move cells simultaneously but it cannot manipulate each cell independently. The beam splitters provide optical tweezers two laser beams and manipulate them individually by the corresponding mirrors. The number of the light in this method, however, is strictly constraint by the number of beam splitters. The last method to construct multiple optical tweezers is using micro mirror array. The system uses a mirror array to reflect incident light and change positions of the light spots by tilting each micro mirror.

Laser guidance can move cells without contact the same as optical tweezers. An objective low numerical aperture is used in the system of laser guidance and provides slightly focused beam.

When the cell passes near the light axis, it will be pulled into the center of the light axis and guided along that direction of the light axis by light pressure [9,10]. A preliminary study shows the manipulation of cells by laser guidance [11]. This method can be also applied to produce micro patterns [12].

In this study, the authors present a method of guiding and tweezing endothelial cells in one system to demonstrate the feasibility of using the same method to build an artificial blood vessel. The diameter of vascular endothelial cells used in the study is about 20–30  $\mu\text{m}$ .

## 2. Design concept

The conceptual design for assembly of vascular endothelial cells is illustrated in Fig. 1, and the schematic diagram of the complete system is shown in Fig. 2. The working processes of the system are as follows. First, the endothelial cells are stored in a syringe and pumped into the main channel in the system. The cells are then guided into branch channels, line up and flow through the channel toward construction area by laser guidance. Thirdly, the optical tweezers trap cells at the end of the branch channel and put them at the proper place to form a piece of blood vessel. Since the scale of blood vessel is much larger than the working area of optical tweezers, the two-step movement of the platform is needed. The coarse manipulation is achieved by moving the micro channel directly on an electromechanical stage and the fine movement is done by laser tweezers.

The optical tweezers are manipulated by tilting the mirror to move the trapped object on the focal plane. The parameters

\* Corresponding author. Tel.: +886 3 5715131; fax: +886 3 5722840.  
E-mail address: [hocheng@pme.nthu.edu.tw](mailto:hocheng@pme.nthu.edu.tw) (H. Hocheng).

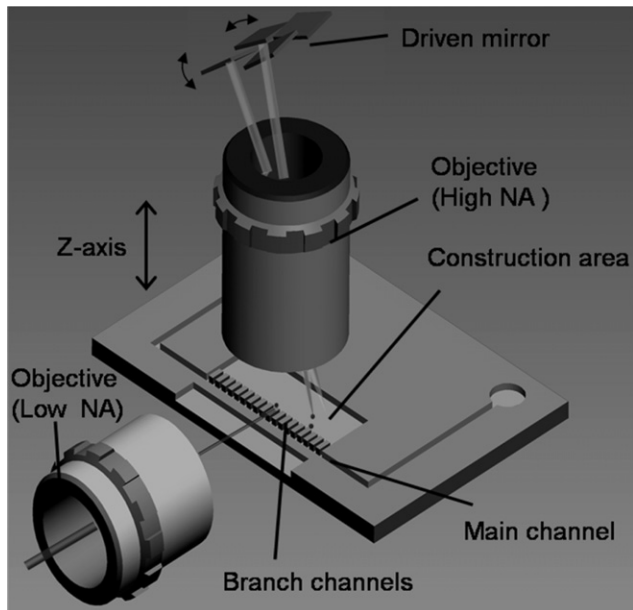


Fig. 1. Conceptual design for assembly of vascular endothelial cells.

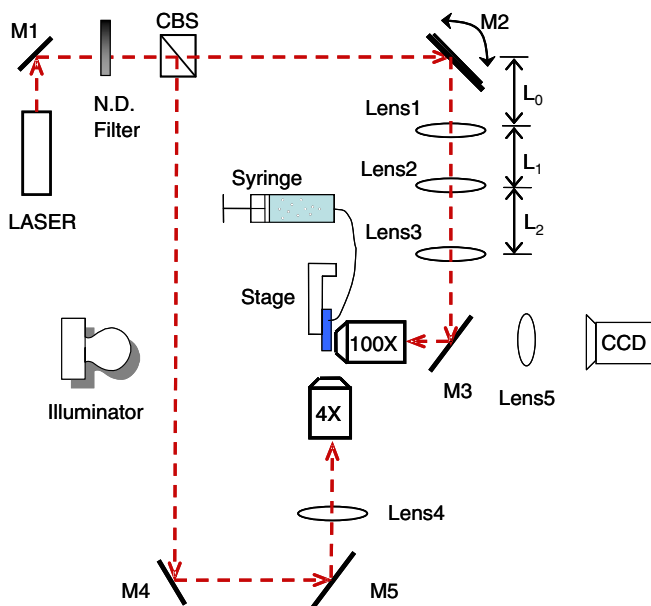


Fig. 2. Schematic diagram of the system setup.

calculated from the paraxial and thin-lens approximations are used as initial conditions and optimized by optics simulation, as discussed in the next section. For the micro channel, the computational fluid dynamics provides the analysis of the geometry of micro channels designed to allow sufficient nutrition entering the construction region so as to keep the cell vital but would not let the flow disturb the assembly process. Based on the analysis in Section 2.2, the proper dimensional parameters are selected to fabricate micro channels in the system.

### 2.1. Optical design

The trapping force of optical tweezers depends on the numerical aperture of the object lens. Higher numerical aperture produces large force. Once a lens is selected, the efficient trapping is

achieved when the entrance pupil of the objective is fully filled by the laser ray all the time along with the mirror tilting. An analysis is conducted to calculate the distance between driven mirror and the lenses.

$$L_0 = \frac{f_1^2}{f_2} + f_1 - \frac{f_1^2}{f_2^2} L_2 + \frac{f_3^2 f_1^2}{f_2^2 x} + \frac{f_3^2 f_1^2}{f_2^2} \quad (1)$$

where  $f_1$ ,  $f_2$  and  $f_3$  are focal lengths of lens1, lens2 and lens3, 38.1 mm, 75.6 mm and 50.2 mm, respectively,  $x$  is the rear conjugate distance of the microscope objective, and  $L_2$  is the distances between lens1 and lens2. If  $L_0$  and  $L_2$  fit this equation, the chief ray height at the entrance pupil of the objective will remain zero in spite of the tilting of the mirror. Because this relation is based on para-axial and thin-lens approximations, these parameters are treated as initial conditions for the optical optimization. Fig. 3 shows the results of the Vignetting analysis of coverage of entrance pupil changing with tilting angle of mirror. The optical simulation software, OSLO, is used for comparison. This software provides more accurate analysis than the para-axial approximation of thin-lens. It shows the entrance pupil can be nearly fully covered for maximal tweezing force when the tilting angle lies between plus and minus  $4^\circ$ .

### 2.2. Micro channel design

The micro channel transfers endothelial cells from outside to the construction area by laser guidance through micro channels. The main channel and the construction area are linked by branch channels. The micro channel should lower the ratio of the fluid flowing into the construction area, defined as the mass flow ratio, which disturbs the cells in that working area. To achieve this goal, three geometric parameters of the micro channel are set, as shown in Fig. 4, namely the width of the main channel,  $A$ , length of branch channels,  $B$ , and widths of branch channels,  $C$ . Fig. 4 shows two designs of the branch channel. In the fluid mechanical analysis,  $A$  and  $B$  for both types vary from  $100 \mu\text{m}$  to  $300 \mu\text{m}$  with increment of  $5 \mu\text{m}$ .  $C$  of nozzle-like branch channel is  $20$  and  $30 \mu\text{m}$ , while  $C$  of straight branch channel varies from  $30$  to  $50 \mu\text{m}$  at a step of  $10 \mu\text{m}$ . A fluidic simulation software CFD-ACE is used to optimize these parameters considering the mass flow ratio of the construction area as the performance index of the simulation. The index of mass flow ratio should be as low as possible.

In the analysis of the flow field, the fluid is considered incompressible and laminar flow. The temperature of the fluid remains constant and the effect of gravity force is neglected. The flow velocity at the inlet of the main channel is  $50 \mu\text{m/s}$ . Fig. 5 and 6 show the results of the analysis. The mass flow ratio of the construction area decreases with the increase of the width of the main channel and the length of the branch channel, and with the decrease of the width of the branch channel. Among these three parameters, the flow behavior mainly depends on the width of the branch channel. In consideration of the size of the endothelial cell, the width of the branch channel is selected  $30 \mu\text{m}$  which is slightly wider than the diameter of the cells.

The fabrication sequence of micro channel is schematically illustrated in Fig. 7. First, a layer of photo resist SU-8 is spin-coated on a  $100 \text{ mm}$  wafer and then exposed to UV light through the photo mask in photolithography. After dissolving the unpolymerized photoresist, a positive relief of the channel structure is left on the wafer; this structure acts as a master for casting PDMS channels. After a master has been fabricated, the surface of the wafer is treated with a layer of Teflon to avoid bonding between the photo resist and PDMS. Using the master, a negative relief of the structure on the master is made in PDMS by replica molding (see Fig. 7c). The replica molding involves pouring PDMS prepolymer

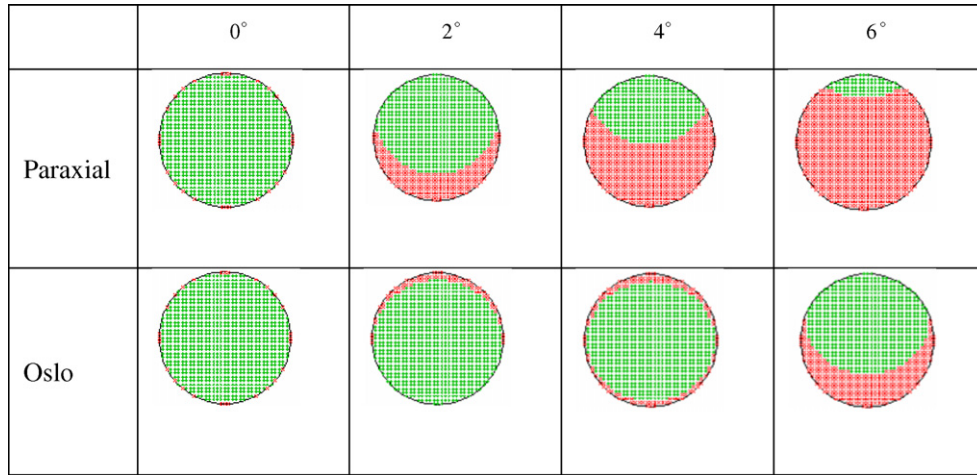
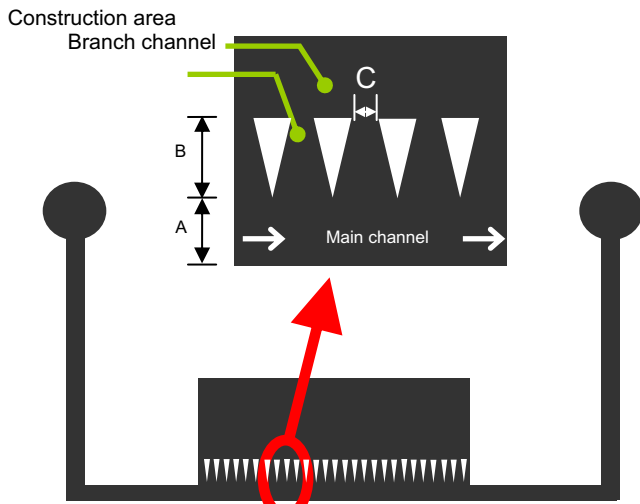
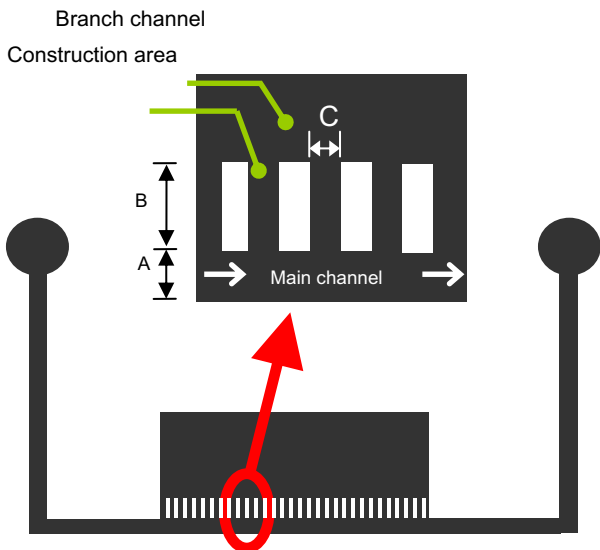


Fig. 3. Vignetting analysis of coverage of entrance pupil.



(a) nozzle-like branch channels



(b) straight branch channels

Fig. 4. Schematic illustration of micro channel.

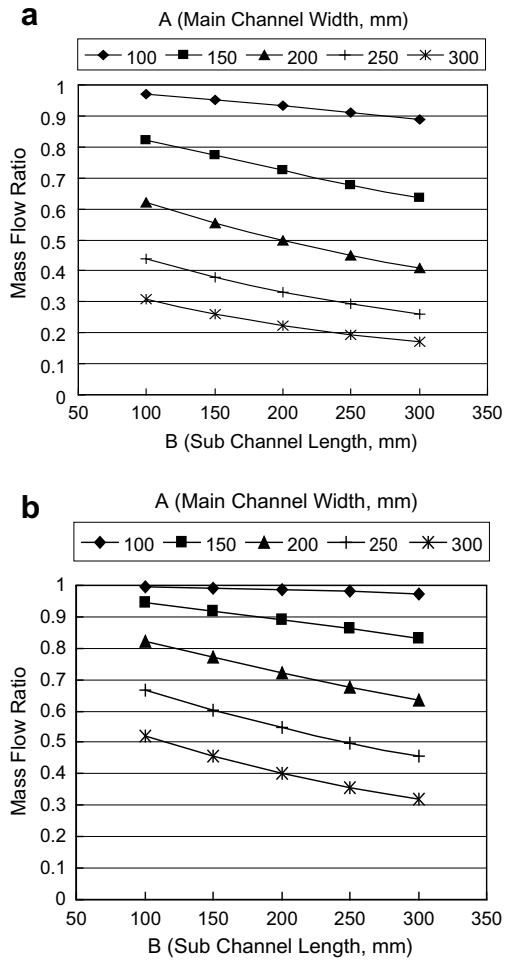
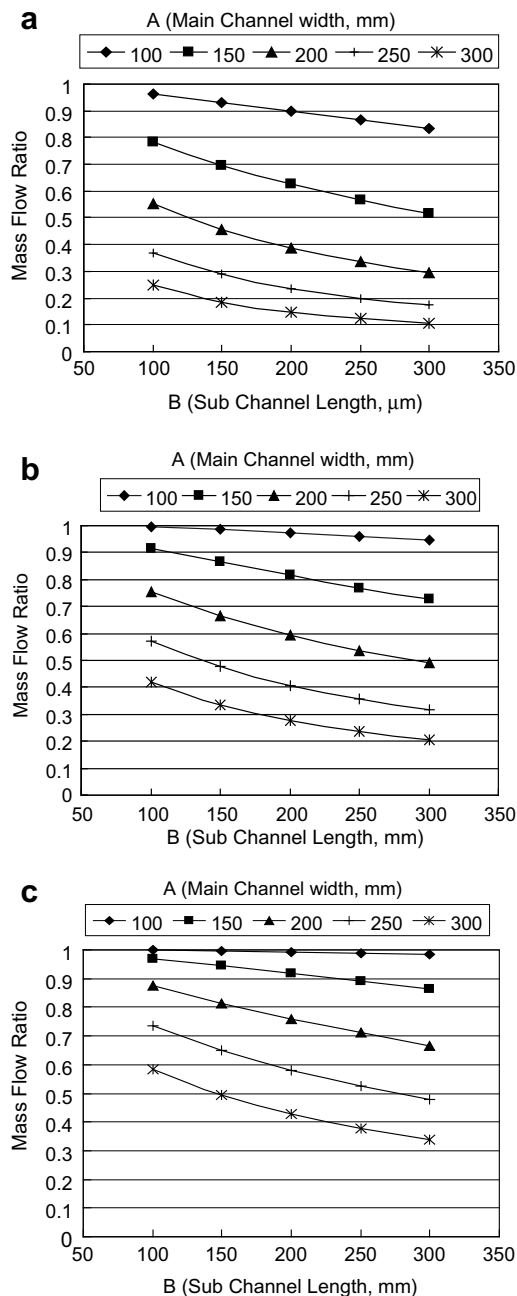


Fig. 5. Simulation of mass flow with different main channel width and branch channel length (a) nozzle-like branch channel width 20 μm and (b) nozzle-like branch channel width 30 μm.

over the master, curing the polymer at 80 °C for 1 h in the oven, and peeling it off the master. Channel inlets and outlets are drilled into the PDMS by a flat-top syringe needle. At last the channel and a piece of cover glass is treated with O<sub>2</sub> plasma simultaneously and then bonded together. Fig. 8 shows the photograph of the micro channel used in the system.



**Fig. 6.** Simulation of mass flow with different main channel width and branch channel length (a) straight branch channel width 30  $\mu\text{m}$ , (b) straight branch channel width 40  $\mu\text{m}$  and (c) straight branch channel width 50  $\mu\text{m}$ .

### 3. Experimental setup

The system layout is shown in Fig. 2. Table 1 shows the specifications of the major components. An infrared laser of wavelength 1064 nm, is used as light source. The laser is divided into two lasers with equal power by a cubic beam splitter (CBS). One light, which is treated as optical tweezers, is reflected by the driven mirror, M2 and goes through the positioned lenses, Lens1, Lens2, Lens3 and then entered an 100 $\times$  objective, sequentially. Another light, which is treated as laser guidance, entered a 4 $\times$  objective. Because PDMS is transparent, the light can pass through it and be focused in the main channel. A CCD is put behind a hot mirror, M3, to observe cells moved by laser guidance and optical tweezers in the micro channel. The micro channel is attached on an electromechanical

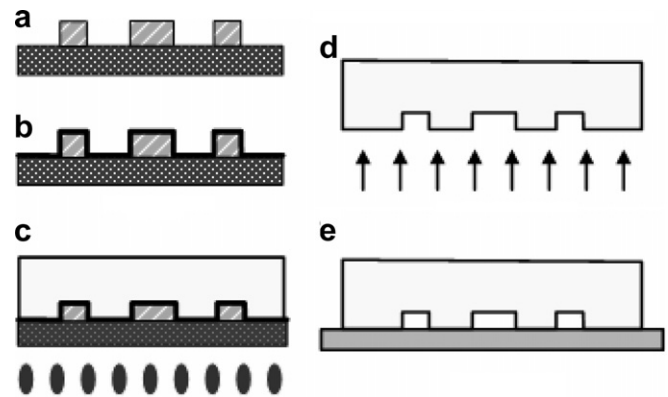


**Fig. 7.** Fabrication sequence of micro channel. (a) Pattern the geometry of micro channel by photo resist, (b) deposit Teflon, (c) pour PDMS on the wafer and heat it, (d)  $\text{O}_2$  plasma treatment and (e) Bonding with glass.

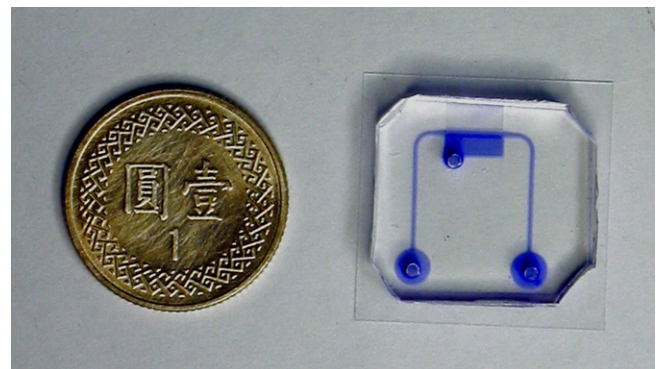


**Fig. 8.** Photograph of microchannel.

stage which provides three-axis translation. The culture medium is stored in the syringe and pumped into micro channel through plastic tube. The polystyrene particles of diameters 6 and 10  $\mu\text{m}$  from poly science are used for manipulation testing in parallel with the cells.

## 4. Results and discussion

### 4.1. Laser guiding

The 10  $\mu\text{m}$  polystyrene micro beads are moved in the main channel and the flow direction is from top to bottom in Fig. 9. The slight focused laser enters the channel from the left side of the channel. When the bead flows into the light axis, the moving direction of the bead turns 90 $^\circ$  to the right. The beads start moving along the light axis and flow through the branch channel into the construction area. The moving speed is several mm per second in that direction. After successfully moving plastic micro beads, endothelial cells are tested in the micro channel. As shown in Fig. 9, three cells are guided into a line by laser beam. The moving speed is lower than the micro beads due to larger size of the cells.

### 4.2. Laser tweezing

An endothelial cell is trapped by laser tweezers and moved horizontally and vertically as shown in Fig. 10. The movement is directed by the tilting mirror. For an oil immersion-type microscope objective with the numerical aperture of 1.25, the working range is a circle of diameter of 70–80  $\mu\text{m}$ . The endothelial cells

**Table 1**  
Specification of optical and associated components

|                     |  |
|---------------------|--|
| Laser               | DPSS laser, wave length = 1064 nm, max power = 1000 mW   |
| Reflector           | Newport 10D10DM.10   |
| Cubic beam splitter | Newport 10BC17MB.2   |
| Hot mirror          | Edmunds F43-956 10D10DM.10   |
| Tweezers lenses     | Newport KPX079AR.33, $f_1 = 38.1$ mm<br>Newport KPX088AR.33, $f_2 = 75.6$ mm<br>Newport KPX082AR.33, $f_3 = 50.2$ mm |
| Laser guidance lens | Newport KPX085, $f_4 = 62.9$ mm  |
| Illuminator         | 30 W Quartz-halogen light  |
| CCD                 | Watec WAT-902H NIR monochrome CCD  |
| Motion stage        | PI M-510.11  |
| Syringe             | KDS 200  |

can be moved at 100  $\mu\text{m/s}$  in use of the laser of around 500 mW. However, the speed is often limited by the actuator response of the tilting mirror.

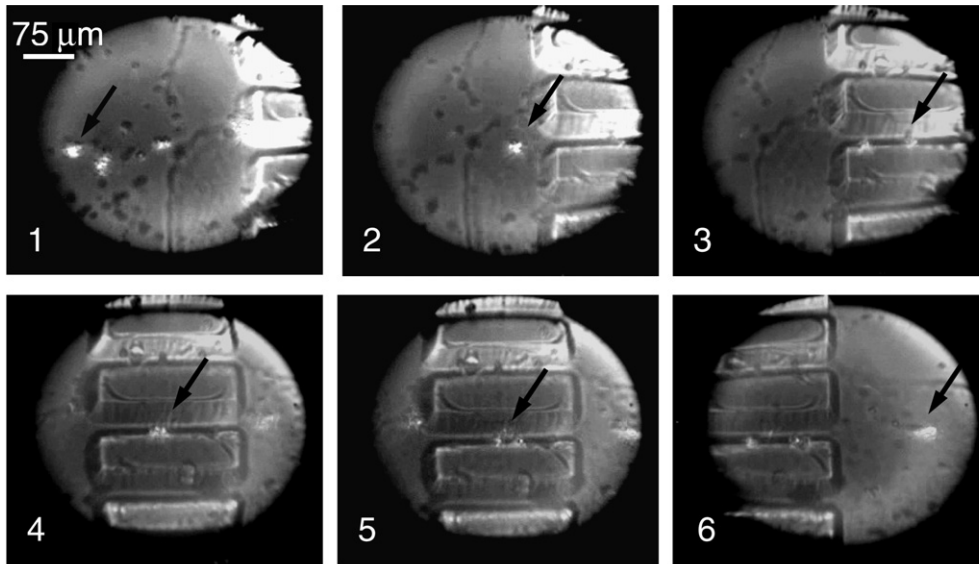
4.3. Escape velocity and laser dragging force

Fig. 11 shows the correlation between laser power and the escape velocity. The escape velocity is measured by moving the positioning stage and observing the trapped object until the object goes off the tweezers at a certain speed. The endothelial cell is larger than the 6  $\mu\text{m}$  polystyrene bead, hence its moving speed is several times lower. It is clear that the higher laser power is, the faster the object can be moved by laser tweezers.

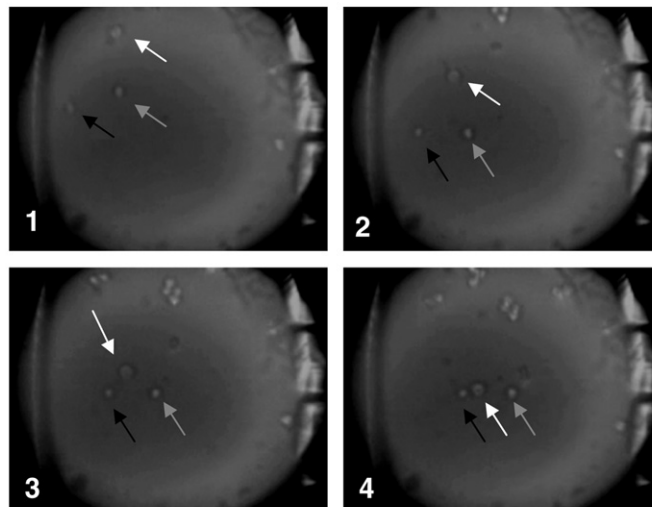
Fig. 12 shows the correlation between laser power and the dragging force. The force is determined by the moving speed and the size of object, and the fluid viscosity based on the Stokes Law. In an infinite and uniform flow field, a sphere is subject to the flow force

$$F = 6\pi\eta Rv \tag{2}$$

where  $\eta$  is fluid viscosity ( $10^{-3}$  N s/m<sup>2</sup> for water),  $R$  is the particle radius,  $v$  is the relative speed of sphere in the flow. Since the lens



(a) a 6  $\mu\text{m}$  polystyrene bead (see the solid arrow) is guided from main channel into construction area through branch channel.



(b) three endothelial cells are guided into a line

Fig. 9. Laser guidance operation.

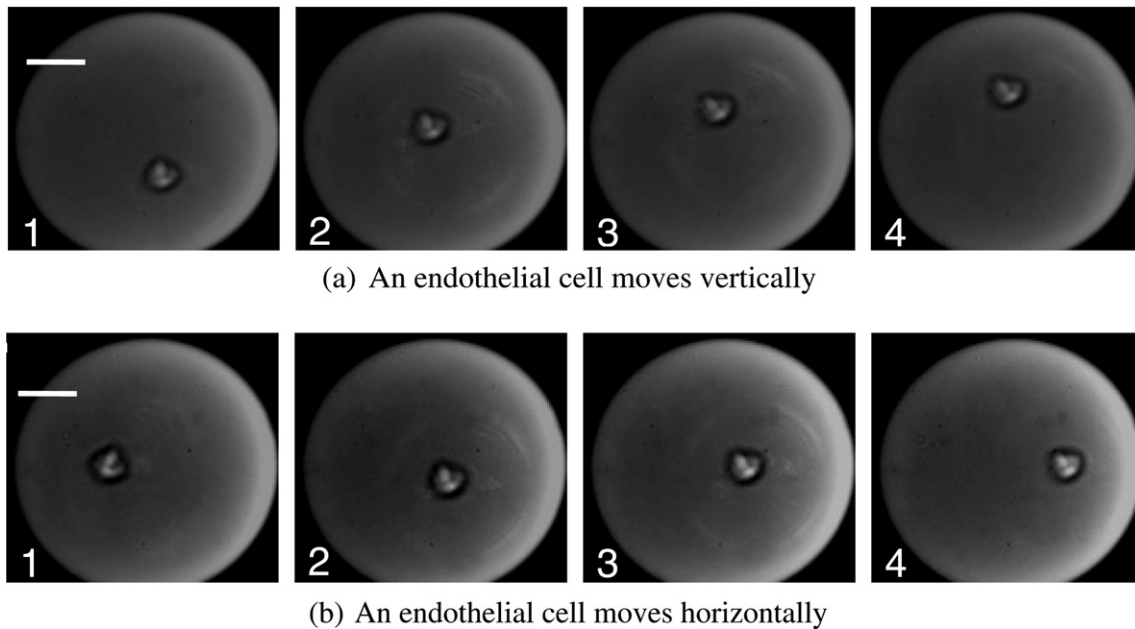


Fig. 10. Laser tweezers operation.

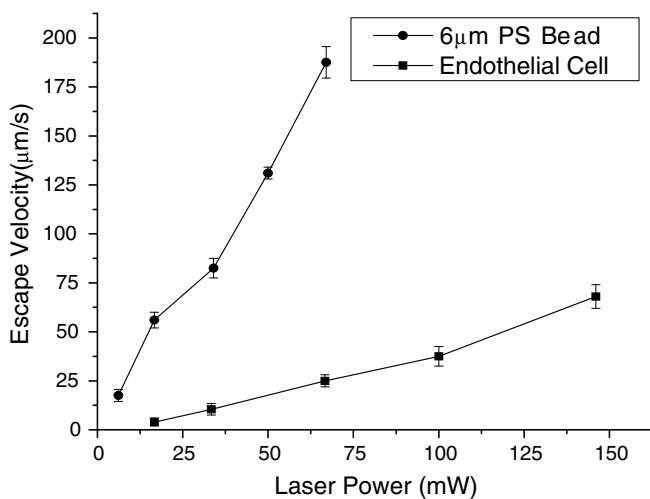


Fig. 11. Correlation between laser power and escape velocity.

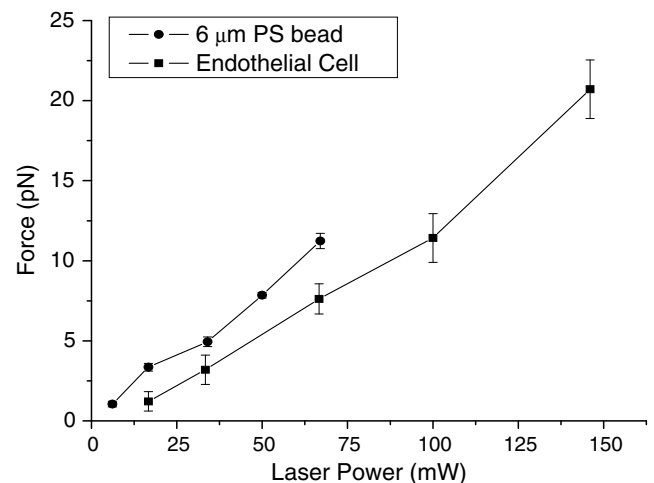


Fig. 12. Correlation between laser power and dragging force.

focus is short thus making the object very close to the lens (around 100 μm), the effective viscosity is increased. The Stokes Law is modified as [13]

$$F = \frac{6\pi\eta Rv}{1 - \frac{9}{16} \left(\frac{R}{h}\right) + \frac{1}{8} \left(\frac{R}{h}\right)^3 - \frac{4}{256} \left(\frac{R}{h}\right)^4 - \frac{1}{16} \left(\frac{R}{h}\right)^5} \quad (3)$$

where  $h$  is the distance between particle and wall. One can see the viscosity increases drastically when the particle size is close to or even larger than  $h$ . In the current study,  $h$  is 30 μm. (The narrowest space in the construction area is 80 μm.) In use of the plastic beads of 6 μm, the viscosity increases 6%, while the endothelial cells of 25 μm will cause an increase of 30%. Thus the modification by Eq. (3) is needed. The larger the object or the narrower the space is, the larger is the drag force. The endothelial cell on one hand has larger size than the polystyrene bead, while on the other hand moves at much lower speed, as shown in Fig. 11. Therefore the dragging force is lower than the bead, as illustrated in Fig. 12. As also expected, the dragging force increases with the applied laser power of the tweezers. The results can be used to design the process of assembling the endothelial cells by the constructed system.

## 5. Conclusion

A system for constructing a blood vessel is proposed. The system is composed of laser guidance, micro channels and laser tweezers. The endothelial cells are first guided from main channel toward the assembly area through the branch channel followed by the laser tweezers moving the cells to the proper place. The main channel should be designed to hundreds of micron meters wide whereas the branch channel should be slightly larger than the size of the cells, to minimize the fluidic disturbance to cells in the assembly area. The position of lenses in the optical path should be designed for the maximum of the effective trapping capability of laser tweezers. Both polystyrene micro beads and endothelial cells are successfully moved by this method. The guiding and tweezing speed for endothelial cells can reach one hundred micron meter per second when laser power level is high and the tilting mirror rotates fast. In the future, the system can operate several laser tools at the same time by replacing the single driven mirror with micro mirror array. More cells can be moved at the

same time and the mirror response is much faster. The assembly process time can be shortened many times.

### Acknowledgments

The current study was supported by Taipei Veteran Hospital under contract VGHUST94-G6-06-4. The authors also appreciate J.W. Hsieh and H.H. Hsu from Instrument Technology Research Center for their technical support for photo lithography.

### References

- [1] A. Ashkin, J.M. Dziedzic, J.E. Bjorkholm, S. Chu, *Opt. Lett.* 11 (1986) 288.
- [2] J.P. Mills, L. Qie, M. Dao, C.T. Lim, S. Suresh, *Mech. Chem. Biosyst.* 1/3 (2005) 169.
- [3] K.C. Neuman, E.H. Chadd, G.F. Liou, K. Bergman, S.M. Block, *Biophys. J.* 77 (1999) 2856.
- [4] R.A. Flynn, A.L. Birkbeck, M. Gross, M. Ozkan, B. Shao, M.M. Wang, S.C. Esener, *Sensors Actuators* 87 (2002) 239.
- [5] E. Fallman, O. Axner, *Appl. Opt.* 36/10 (1997) 2107.
- [6] E.R. Dufresne, G.C. Spalding, M.T. Dearing, S.A. Sheets, D.G. Grier, *Rev. Sci. Instrum.* 72/31 (2001) 1810.
- [7] J.E. Curtis, B.A. Koss, D.G. Grier, *Opt. Commun.* 207 (2002) 169.
- [8] N.G. Dagalakis, T. LeBrun, J. Lippiatt, in: *Conference of IEEE-Nano (Academic 2002)*, p. 177.
- [9] M.J. Renn, R. Pastel, H.J. Lewandowski, *Phys. Rev. Lett.* 82/7 (1999) 1574.
- [10] D.J. Odde, M.J. Renn, *Biotechnol. Bioeng.* 67/3 (2000) 312.
- [11] H. Hocheng, C. Tseng, in: *5th World Congress of Biomechanics, (Academic 2006) Munich, Germany.*
- [12] H. Hocheng, C.H. Liao, in: *ROC patent 257964 and USA patent pending, (Academic 2006) 0121641-A1.*
- [13] K. Svoboda, S.M. Block, *Annu. Rev. Biophys. Biomol. Struct.* 23 (1994) 247.